JOURNAL OF SOLID STATE CHEMISTRY **125,** 112–115 (1996)
ARTICLE NO. 0272

LETTER TO THE EDITOR

Determination of Mn Valence from X-Ray Absorption Near Edge Structure and Study of Magnetic Behavior in Hole-Doped $(Nd_{1-x}Ca_x)MnO_3$ System

R. S. Liu, J. B. Wu, and C. Y. Chang

Department of Chemistry, National Taiwan University, Taipei, Taiwan, Republic of China

J. G. Lin and C. Y. Huang

Center for Condensed Matter Sciences and Department of Physics, National Taiwan University, Taipei, Taiwan, Republic of China

and

J. M. Chen and R. G. Liu

Synchrotron Radiation Research Center, Hsinchu, Taiwan, Republic of China

Communicated by J. M. Honig, May 7, 1996; accepted June 11, 1996

The Mn valence in $(Nd_{1-x}Ca_x)MnO_3$ ($x = 0$–0.5) has been successfully determined using Mn 2_p-edge X-ray absorption near edge structure spectra. Moreover, we have measured the magnetic properties across the series $(Nd_{1-x}Ca_x)MnO_3$; the results show that the perovskite $NdMnO_3$ is an antiferromagnet with two Néel temperatures (T_N) of 14 and 60 K, respectively. By replacement of Nd^{3+} with Ca^{2+}, the mixed compounds $(Nd_{1-x}Ca_x)MnO_3$ became ferromagnetic with a Curie temperature of around 130 K (T_C) for x in the range 0.1–0.3. Furthermore, two weak antiferromagnetic transitions with T_N's of around 30 and 75 K, respectively, embedded in the matrix of the ferromagnet have also been discovered in the range $x = 0.2$–0.3. For $x \geq 0.4$, the samples change to antiferromagnetic with T_N's of around 30 K together with a weak broad ferromagnetic transition with T_C's of around 130 K. It is also important to note that the charge-ordering-induced antiferromagnetic transition at the temperature (T_{CO}) 250 K was observed in the samples of $x = 0.4$ and 0.5.

1. INTRODUCTION

Recently considerable attention has been attracted to the observation of giant magnetoresistance (GMR) in films (1–3) and single crystals (4, 5), as well as in polycrystalline pellets (6–10) of hole-doped $LnMnO_3$ with the general chemical composition $Ln_{1-x}A_xMnO_3$ (Ln = rare earth; A = Pb, Ba, Sr, Ca). It is known that partial chemical replacement of Ln^{3+} ions with 2+ valence ions (A) such as Pb, Ba, Sr, and Ca in $Ln_{1-x}A_xMnO_3$ can lead to strong ferromagnetism and metallic conductivity for x around 0.3. This results in a Mn^{3+}/Mn^{4+} mixed valence state that creates mobile charge carriers (holes) and canting of Mn spins. The resistivity drop of these materials due to an external magnetic field is usually much larger than that observed in magnetic multilayers (11, 12). Large magnetoresistance is of current interest due to the possibility of producing devices (especially in magnetic recording heads) which make use of this effect.

The ferromagnetic ground state of metallic $Ln_{1-x}A_xMnO_3$ is caused by the so-called "double exchange" interaction between the Mn^{3+} and Mn^{4+} ions. Therefore, the determination of the valence of Mn ions in $Ln_{1-x}A_xMnO_3$ becomes important in understanding the mechanism of interplay between magnetic and conducting properties. Conventional redox titration (e.g., using potassium permanganate and ferrous sulfate) by dissolving the samples in adequate solvent is widely used for this purpose. Here, we demonstrate a nondestructive method for determining the valence of Mn in $(Nd_{1-x}Ca_x)MnO_3$ ($x = 0$–0.5) by using Mn $2p$-edge X-ray absorption near edge structure (XANES) spectra. Moreover, the magnetic transition induced by the variation of the chemical substituent x in $(Nd_{1-x}Ca_x)MnO_3$ will also be reported.

0022-4596/96 $18.00

2. EXPERIMENTAL

High purity powders of Nd_2O_3, MnO_2, and CaO were weighed in the appropriate proportions to constitute the nominal compositions of $(Nd_{1-x}Ca_x)MnO_3$ (x = 0–0.5). The mixture was first heated in air to 900°C for 12 hr. The preheated powders were then ground and pressed into a pellet (15 mm in diameter and 3 mm in thickness) under a pressure of 5 ton/cm^2. The pellets were then sintered at 1200°C for 12 hr in air. After sintering, the furnace was cooled to room temperature at a rate of 5°C/min. The X-ray diffraction analyses carried out with a Phillips diffractometer (Cu$K\alpha$ radiation) show that the materials across the series crystallize as a pure phase. The valence of Mn was determined by the X-ray absorption technique. The X-ray absorption measurements were carried out on the 6 m high-energy sphere grating monochromator (HSGM) beamline of the Synchrotron Radiation Research Center (SRRC) in Taiwan. During the measurements, the energy resolution of the monochromator was set to about 0.25 eV at the Mn 2p edge (~640 eV). The photon energies were calibrated within an accuracy of 0.1 eV via the known OK edge absorption peak of CuO. The magnetic properties of the samples were measured (zero-field cooled) in an applied magnetic field of 1000 G using a Quantum Design (MPMS) SQUID magnetometer.

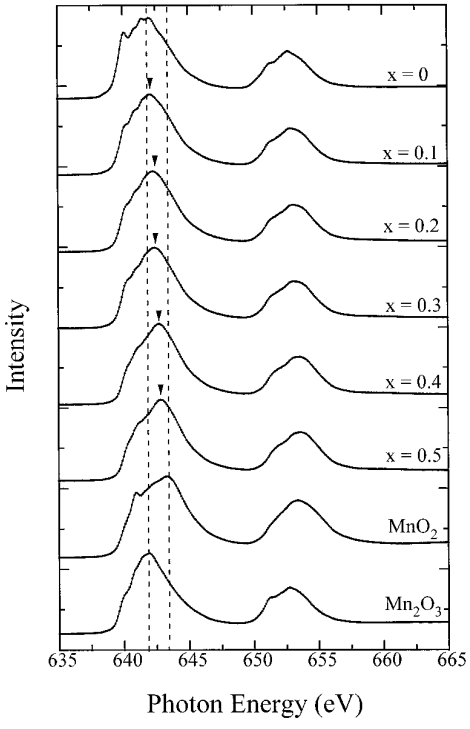

FIG. 1. The Mn 2p-edge X-ray absorption near edge structure (XANES) spectra of $(Nd_{1-x}Ca_x)MnO_3$ (x = 0–0.5), MnO_2 (Mn^{4+}), and Mn_2O_3 (Mn^{3+}).

3. RESULTS AND DISCUSSION

The Mn 2p-edge X-ray absorption near edge structure (XANES) spectra of $(Nd_{1-x}Ca_x)MnO_3$ for various Ca concentrations are shown in Fig. 1. For comparison, the Mn 2p X-ray absorption spectra of MnO_2 (Mn^{4+}) and Mn_2O_3 (Mn^{3+}) are also plotted in Fig. 1. As seen from Fig. 1, the spectra show two broad multiplet structures separated by spin–orbit splitting. Furthermore, when Nd^{3+} is replaced by Ca^{2+} in $(Nd_{1-x}Ca_x)MnO_3$, the Mn 2p spectra change shape and shift toward higher energies, as indicated in Fig. 1. In particular, the maximum of the $Mn_{3/2}$ multiplet in Fig. 1, marked by arrows, moves from 641.8 eV in $NdMnO_3$ to 643.3 eV in $(Nd_{0.5}Ca_{0.5})MnO_3$. The change of the spectral shape is due to the variation in symmetry of the ground state (13). The chemical shift is caused by changes in the electrostatic energy at the Mn site driven by the variation of the ionic valence in the compounds. It is well established that the effective ionic valence of the compounds can be measured from the chemical shift of the core-level X-ray photoemission spectroscopy (14, 15). However, it has been also experimentally shown that the chemical shift of the first unoccupied excited state in the core-level X-ray absorption spectrum is related to the effective ionic valence (16, 17). Recently, these chemical shifts in electron energy loss spectroscopy (EELS) were also used to determine the valences of the transition-metal based compounds (18). We therefore adopt the same scheme to obtain the Mn valence in the system studied. A plot of the ionic valence of Mn versus x in $(Nd_{1-x}Ca_x)MnO_3$ reveals a linear correlation. This proved that holes can be efficiently induced and increased in the Mn sites with increasing x (i.e., Ca^{2+} substituting for Nd^{3+}) in $(Nd_{1-x}Ca_x)MnO_3$. As demonstrated in Fig. 1, the main peak position of the Mn 2p-edge in $NdMnO_3$ is closer to that in Mn_2O_3 with Mn^{3+} in a slightly distorted octahedral symmetry. The valence of Mn in the $(Nd_{1-x}Ca_x)MnO_3$ system increases with increasing Ca concentration. This leads to the conclusion that the chemical shifts of the absorption peak in X-ray absorption spectra could be deduced from charge variations when difficult or nearly impossible to calculate.

In Fig. 2, we show the temperature dependence of the magnetization at a magnetic field of 1000 G for the series of the $(Nd_{1-x}Ca_x)MnO_3$ (x = 0–0.5) compounds. The parent $NdMnO_3$ compound is an antiferromagnet with two Neel temperatures of around 14 and 60 K, respectively (as shown in Fig. 2). The $NdMnO_3$ compound contains Mn^{3+} ions with $t_{2g}^3e_g^1$ (spin quantum number S = 2) configuration. This is confirmed by the X-ray absorption from the main peak position of the Mn 2p-edge in the $NdMnO_3$ compound which is near that in Mn_2O_3 with Mn^{3+} in a slightly distorted octahedral symmetry (as shown in Fig. 1). The t_{2g} electrons are localized and so can be regarded as local

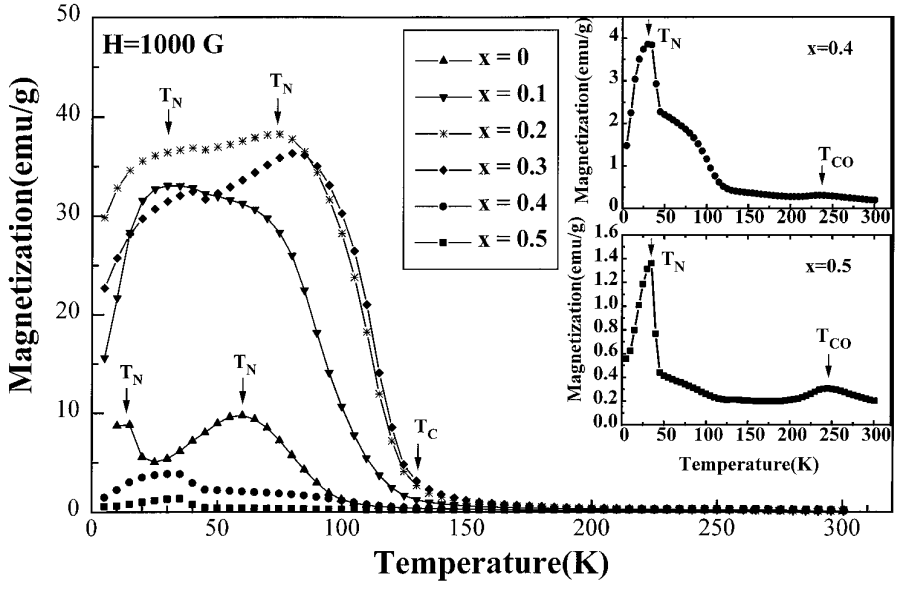

FIG. 2. Temperature dependence of magnetization at a magnetic field of 1000 G for the series of the $(Nd_{1-x}Ca_x)MnO_3$ ($x = 0$–0.5) compounds.

spins with $S = \frac{3}{2}$. In contrast, the e_g electrons in Mn^{3+} are strongly hybridized with the oxygen $2p$ state and cause antiferromagnetic superexchange coupling. However, the reason for the observation of two T_N's in $(Nd_{1-x}Ca_x)MnO_3$ is still unclear, which may be due to the phase transformation at these two temperatures or to the contribution from the magnetic spins from the Nd^{3+} ions coupling with that from the Mn^{3+} ions. For $0.1 \leq x \leq 0.3$, the $(Nd_{1-x}Ca_x)MnO_3$ samples change from the antiferromagnetic state into the ferromagnetic state with T_C's of around 130 K (see Fig. 2). This may be because the chemical substitution of Sr^{2+} for La^{3+} introduces holes into the e_g orbitals (e.g., an increase in the valence of Mn above 3+) that are mobile and mediate an interatomic ferromagnetic interaction between the Mn atoms; the e_g electrons procure kinetic energy through the so-called ''double-exchange interaction'' (19, 20). Recently, such a strongly spin–charge coupled state has been extensively reexamined in light of the observation of an enormous magnetoresistive effect (1–10). Furthermore, two weak antiferromagnetic components with Néel temperatures (T_N) of around 30 and 75 K, respectively, embedded in the matrix of the ferromagnet have also been found in the range $x = 0.2$–0.3. Such behavior may correspond to the exhibition of multiple intermediate phases at such low temperatures. For $x \geq 0.4$, the samples change to antiferromagnetic with T_N's of around 30 K together with a weak broader ferromagnetic part with T_C's of around 130 K as shown in Fig. 2. Moreover, the charge-ordering-induced antiferromagnetic transition at the temperature (T_{CO}) 250 K was observed in the samples of $x = 0.4$ and 0.5 (more pronounced at $x = 0.5$), as indicated in the insets of Fig. 2. This is contributed from the ordering of the Mn ions into a Mn^{3+}/Mn^{4+} sublattice at compositions near 50% doping. A similar effect has been observed in the $(Pr_{1-x}Sr_x)MnO_3$ (21), $(Pr_{1-x}Ca_x)MnO_3$ (22), and $(La_{1-x}Ca_x)MnO_3$ (23) systems with T_{CO}'s of 140, 250, and 170 K, respectively, for $x \sim 0.5$. The application of a magnetic field can melt this charge ordering state, leading to a large decrease in resistivity and a ferromagnetic state (21, 22). More details about the relationship between the magnetic transition and phase transformation with variation of temperature in $(Nd_{1-x}Ca_x)MnO_3$ are currently being investigated.

ACKNOWLEDGMENTS

The work is supported by the National Science Council of the Republic of China under the Grants NSC-2112-M-002-022 and NSC-2112-M-002-023.

REFERENCES

1. K. Chahara, T. Ohno, M. Kasai, and Y. Kozono, *Appl. Phys. Lett.* **63,** 1990 (1993).
2. R. von Helmolt, J. Wecker, B. Holzapfel, L. Schultz, and K. Samwer, *Phys. Rev.* **71,** 2331 (1993).
3. S. Jim, T. H. Tiefel, M. McCormack, R. A. Fastnacht, R. Ramesh, and L. H. Chen, *Science* **264,** 413 (1994).
4. R. M. Kusters, J. Singleton, D. A. Keen, R. McGreevy, and W. Hayes, *Physica B* **155,** 362 (1989).
5. A. Anane, C. Dupas, K. L. Dang, J. P. Renard, P. Veillet, A. M. de L. Guevara, F. Millot, L. Pinsard, and A. Revcolevschi, *J. Phys. Condens. Matter* **7,** 7015 (1995).
6. S. Jin, H. M. O'Bryan, T. H. Tiefel, M. McCormack, and W. W. Rhodes, *Appl. Phys. Lett.* **66,** 382 (1995).

7. R. Mahesh, R. Mahendiran, A. K. Raychaudhuri, and C. N. R. Rao, *J. Solid State Chem.* **114,** 297 (1995).
8. B. Raveau, A. Maignan, and V. Caignaert, *J. Solid State Chem.* **117,** 424 (1995).
9. R. Mahesh, R. Mahendiran, A. K. Raychaudhuri, and C. N. R. Rao, *J. Solid State Chem.* **120,** 204 (1995).
10. R. Mahendiran, S. K. Tiwary, A. K. Raychaudhuri, and T. V. Ramakrishnan, R. Mahesh, N. Rangavittal, and C. N. R. Rao, *Phys. Rev. B* **53,** 3348 (1996).
11. M. N. Baibich, J. M. Broto, A. Fert, F. Nguyen Van Dau, F. Petroff, P. Eitenne, G. Creuzet, A. Friederich, and J. Chazelas, *Phys. Rev. Lett.* **61,** 2472 (1988).
12. S. S. P. Parkin, N. More, and K. P. Roche, *Phys. Rev. Lett.* **64,** 2304 (1990).
13. F. M. F. de Groot, J. C. Fuggle, B. T. Thole, and G. A. Sawatzky, *Phys. Rev. B* **41,** 928 (1990).
14. K. Siegbahn, C. Nordling, G. Johansson, J. Hedman, P. F. Heden, K. Hamrin, U. Gelius, T. Berkmark, L. O. Werme, R. Manne, and Y. Baer, ''ESCA Applied to Free Molecules,'' North Holland, Amsterdam, 1971.
15. T. A. Carlson, ''Photoelectron and Auger Spectroscopy,'' Plenum, New York, 1975.
16. J. Stohr, ''NEXAFS Spectroscopy,'' Spring-Verlag, New York, 1992.
17. A. Bianconi, *in* ''X-ray Absorption: Principles, Applications, Techniques of EXAFS, SEXAFS, and XANES'' (D. C. Koningsberger and R. Prins, Eds.), p. 573. Wiley, New York, 1988.
18. Taftø and O. L. Krivanek, *Phys. Rev. Lett.* **48,** 560 (1982).
19. C. Zener, *Phys. Rev.* **82,** 403 (1951).
20. J. B. Goodenough, *Phys. Rev.* **100,** 564 (1955).
21. Y. Tomioka, A. Asamitsu, Y. Moritomo, H. Kuwahara, and Y. Tokura, *Phys. Rev. Lett.* **74,** 5108 (1995).
22. M. R. Lees, J. Barratt, G. Balakrishnan, and D. McK. Paul, *Phys. Rev. B* **52,** R14303 (1995).
23. P. G. Radaelli, D. E. Cox, M. Marezio, S.-W. Cheong, P. E. Schiffer, and A. P. Ramirez, *Phys. Rev. Lett.* **75,** 4488 (1995).